ELASTIC γP SCATTERING AT 40 — 70 MEV AND THE POLARIZABILITY OF THE PROTON

V. I. GOL'DANSKIĬ, O. A. KARPUKHIN, A. V. KUTSENKO, and V. V. PAVLOVSKAYA

P. N. Lebedev Physics Institute, Academy of Sciences, U.S.S.R.

Submitted to JETP editor January 12, 1960

J. Exptl. Theoret. Phys. (U.S.S.R.) **38**, 1695-1707 (June, 1960)

Elastic γp scattering at 40 to 70 Mev is investigated and the differential cross sections at 45, 75, 90, 120, 135, and 150° are determined. The results obtained are compared with the theory that takes into account the anomalous proton magnetic moment as well as the effect of mesic cloud polarization. The cross section of γp scattering at 90° corresponds to a proton electric polarizability $\alpha_E = (11 \pm 4) \times 10^{-43}$ cm^3. In addition to the experimental results, we use the dispersion relations with which the value of the sum of the electric (α_E) and magnetic (α_M) polarizabilities can be obtained from the π-photoproduction data: $\alpha_E + \alpha_M = 11 \times 10^{-43}$ cm^3. With account of this value, the obtained experimental data correspond to the following values of the proton polarizabilities:

$$\alpha_E = (9 \pm 2) \cdot 10^{-43} \text{cm}^3, \quad \alpha_M = (2 \mp 2) \cdot 10^{-43} \text{cm}^3$$

Corresponding to the value obtained for the electric polarizability is an rms fluctuation of the proton electric dipole length $(\overline{r^2})^{1/2}$ = (3.5 to 5) × 10^{-14} cm.

1. INTRODUCTION

THE elastic scattering of γ quanta by protons differs radically from the well-known Compton effect on electrons. The difference is due primarily to the anomalous magnetic moment of the proton. The scattering of γ quanta by spin-½ particles was considered in its general form by Pauli. The theory of such scattering was subsequently developed by Powell,[1] Gell-Mann and Goldberger,[2] Low,[3] Klein,[4] and Capps.[5] The scattering amplitude obtained in references 2 to 5 includes, along with the Thomson term, also additional terms linear in the frequency of the γ quantum.

The γp scattering cross section in the laboratory system (l. s.), accurate to terms of order γ^2 (where $\gamma = h\nu/Mc^2$ and M is the proton mass) is given by a formula similar to that of Powell:

$$\frac{d\sigma}{d\Omega}(\theta) = \frac{1}{2} r_0^2 \{[1 - 2\gamma(1 - \cos\theta) + 3\gamma^2(1 - \cos\theta)^2](1 + \cos^2\theta) + \gamma^2[(1 - \cos\theta)^2 + f(\theta)]\}, \quad (1)$$

where $r_0 = e^2/Mc^2$, and the role of the anomalous magnetic moment is characterized by the term

$$f(\theta) = a_0 + a_1 \cos\theta + a_2 \cos^2\theta. \quad (2)$$

The coefficients a_0, a_1 and a_2 are power functions of the anomalous part of the proton anomalous magnetic moment $\lambda_a = 1.7896$. Their values are

$$a_0 = 2\lambda_a + \tfrac{9}{2}\lambda_a^2 + 3\lambda_a^3 + \tfrac{3}{4}\lambda_a^4 = 42.88, \quad (3)$$

$$a_1 = -4\lambda_a - 5\lambda_a^2 - 2\lambda_a^3 = -34.63, \quad (4)$$

$$a_2 = 2\lambda_a + \tfrac{1}{2}\lambda_a^2 - \lambda_a^3 - \tfrac{1}{4}\lambda_a^4 = -3.12. \quad (5)$$

It is obvious that the presence of the anomalous magnetic moment leads not only to an overall increase in the scattering cross section, but also to definite change in the type of angular distribution, viz: to an increase in the fraction scattered in the backward hemisphere.

Effects due to the anomaly of the magnetic moment are by far not the only feature of scattering of γ quanta by protons. The presence of the meson cloud makes possible a direct interaction between the γ quanta and this cloud. This manifests itself not only in the photoproduction of pions, but also in scattering. The Thomson cross section of $\gamma\pi^+$ scattering is 45 times greater than that of γp scattering, and the meson effects should greatly influence the γp scattering picture not only near the photoproduction threshold, but even at much lower energies.

The absorption of γ quanta leads to polarization of the meson cloud and induces in the proton electric and magnetic dipoles which give rise to secondary radiation. This, for example, is the cause of Rayleigh scattering, well known from optics, the role of which in the Compton effect on protons was

noted by Capps[5] and considered in detail by A. M. Baldin,[5] who investigated the influence of proton polarizability on the γp scattering.

The amplitude of the Rayleigh scattering is proportional to the square of the γ-quantum frequency, the proportionality constants for the electric and magnetic dipole transitions being the electric and magnetic polarizability constants of the protons. These characterize both the ability of the meson clouds to become deformed under the influence of the external electric and magnetic fields, and the static distribution of the electric charge and the magnetic moment. The question of a possible delineation of the roles of these different phenomena will not be considered here. The term 'polarizability' used here is therefore not equivalent to the one normally employed for neutral particles, a fact that must be kept in mind throughout.

Although the scattering-amplitude terms due to the proton polarizability are proportional to the square of the frequency, they interfere only with the constant Thomson term, and lead therefore to terms quadratic in the frequency in the formula for the scattering cross section. Confining ourselves to similar quadratic terms in the cross section for γp scattering, we arrive at the following expression for the differential cross section of the Rayleigh-Powell γp scattering, in the l.s.,

$$d\sigma/d\Omega = \tfrac{1}{2} r_0^2 \{[1 - 2\gamma(1 - \cos\theta) + 3\gamma^2(1 - \cos\theta)^2 - 2A_E\gamma^2](1 + \cos^2\theta) - 4A_M\gamma^2\cos\theta + \gamma^2[(1 - \cos\theta)^2 + f(\theta)]\}, \quad (6)$$

where $f(\theta)$ is defined by (2), and the dimensionless factors A_E and A_M represent the polarizabilities α_E and α_M, expressed in units $(e^2/\hbar c)(\hbar/Mc)^3 = 6.8 \times 10^{-44}\,cm^3$.

As shown by V. A. Petrun'kin (private communication), Eq. (6) can be rigorously derived from the dispersion relations at low frequencies. In the interpretation of γp scattering experiments at energies much lower than the photomesic threshold (when $\gamma \ll 1$), use can be made of Eq. (6), in which two parameters, the electric and magnetic polarizabilities of the proton, must be determined experimentally. It is clear that at low energies the proton polarization causes only a slight difference between (6) and (1), if the latter is limited to terms proportional to γ^2. Therefore, in spite of the relative simplicity of the theoretical interpretation of the results, the accuracy requirements imposed on the experiment will be more stringent than in investigations of harder γ quanta.

The purpose of the present investigation was to ensure as high an experimental accuracy as possible, so that experiments on scattering of γ quanta of energy 40 — 70 Mev by protons could yield data on the polarizability of protons.

2. EXPERIMENTAL PROCEDURE

The experiments were carried out with the 265-Mev synchrotron of the Physics Institute of the Academy of Sciences, at a maximum bremsstrahlung spectrum energy of 75 Mev, i.e., at energies much below the threshold of photoproduction of π^0 mesons. Since only the scattered γ quanta need be recorded at these energies (without coincidence with the recoil protons), we used a target large enough to ensure a γp-scattering counting rate on the order of 0.5 or 1 pulse/minute.

Target. A diagram of the setup is shown in Fig. 1. The bremsstrahlung beam from the synchrotron was collimated and made to strike a liquid-hydrogen target. The working part of the target was a cylindrical vessel, elongated in the direction of the beam axis (12 cm dia., 30 cm long), approximately 3.5 l in capacity, filled with liquid hydrogen. Double walls of foamed polystyrene (PS-4) of approximate density 40 mg/cm^3 made up a cavity 1 cm deep in the unexposed part of the target. This cavity was filled with liquid nitrogen. The total capacity of the target vessel (~ 8.5 l of liquid hydrogen) ensured, at an average rate of evaporation of ~ 0.6 l/hr, continuous operation for approximately eight hours without refilling. The chosen working length of the target kept its exposed walls from entering the "field of view" of the detecting telescopes (except in the experiments at 150°), thus reducing considerably the background due to the unfilled target.

Detector. The high-threshold (~ 35 Mev) γ-quantum detectors used were two telescopes, consisting of three scintillation counters (terphenyl in toluol, 3 g/l), with a lead converter past the first counter and an aluminum absorber ahead of the last one (Fig. 1). Each counter was provided with a FÉU-33 photomultiplier. The photomultipliers operated in a specially selected mode ($E_{FÉU}$ = 3 to 4 kv), producing output pulses of 30 — 40 v amplitude from a Co^{60} source when operating directly into an RK-50 cable. It was thus possible to dispense with further amplification of the pulses from the photomultipliers.

Paraffin absorbers 5 or 7 cm thick were placed at the inputs of the telescope channels, to reduce the loading of the first counter, A, by soft electrons and γ quanta.

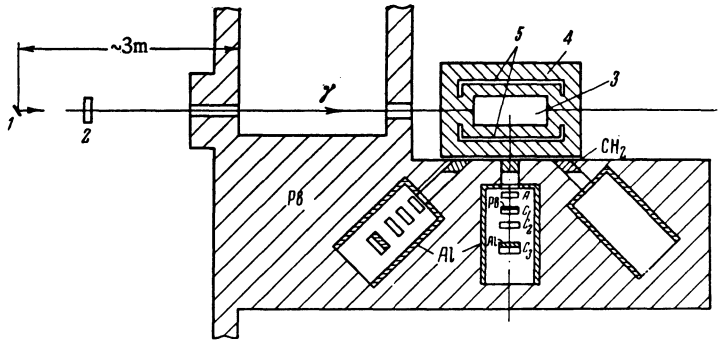

FIG. 1. Diagram of experimental setup: 1 – synchrotron target, 2 – monitor, 3 – liquid-hydrogen target, 4 – polystyrol walls, 5 – liquid nitrogen, C_1, C_2, C_3 – scintillation counters connected for coincidence, A – anticoincidence counter.

Electronic Circuitry. A block diagram of the electronic apparatus used in the experiment is shown in Fig. 2. A few additional explanations are in order. Two fast coincidence circuits of the parallel type with D2V germanium diodes were used. The first discriminator (D_1), used to reduce the load of the slow circuits, was temperature-compensated for threshold drift. The second discriminator (D_2) is the one developed by Park[7], so that a low-gain amplifier can be used. The shaped pulses from both coincidence circuits were fed to a slow anticoincidence circuit, which excluded the count due to charged particles. The possibility of simultaneous registration of the readings in all three channels made for convenient monitoring of the individual circuit elements.

The outputs of the two coincidence circuits and of the anticoincidence circuit were fed to transmission circuits controlled by the accelerator. The readings were registered only during a time interval somewhat longer than the duration of the intensity pulse from the synchrotron, thereby reducing the cosmic-ray background (by about 50). It was also possible to apply a signal to prevent registration of the readings whenever the character of the synchrotron pulses changed.

Monitors. The intermediate monitor used was a thin-wall ionization chamber, placed ahead of the first collimator. All the measurements were reduced to a definite number of counts in this chamber. The absolute value of the energy flux passing through the collimator for a given number of monitor counts was regularly determined from the activity of standardized carbon detectors in the reaction $C^{12}(\gamma, n)C^{11}$, the cross section of which is known.[8,9] The detectors were placed at the center of the target. To make the absolute calibration of the monitor more precise, data on the activation of the carbon were periodically compared with the readings of a thick-walled graphite chamber with a known absolute sensitivity (so-called Lax chamber). The values of the γ-quantum flux obtained by the two methods coincided within approximately 3%.

Experimental Conditions. The electron pulses from the synchrotron were stretched to approximately 300 μsec, corresponding to a change in maximum energy of the bremsstrahlung spectrum from 62 to 75 Mev. The shape of the pulse (approximately rectangular) was monitored visually with the aid of an IO-4 oscillograph synchronized with the accelerator.

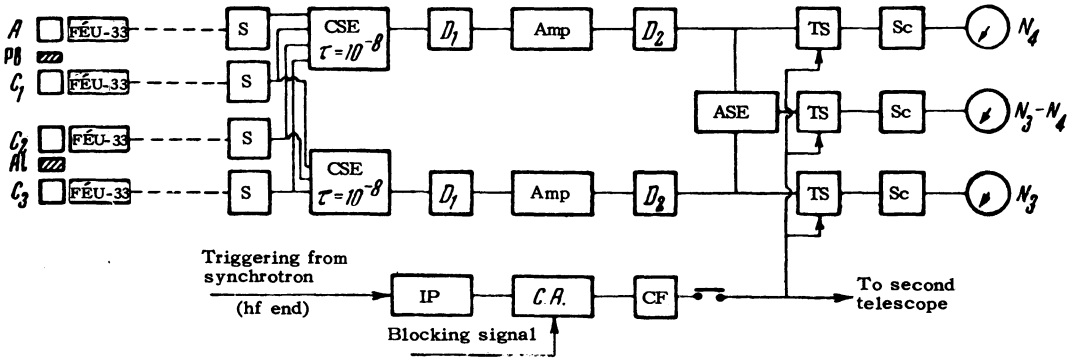

FIG. 2. Block diagram of the electronic apparatus: C_1, C_2, C_3, A – scintillation counters, S – pulse shaping, CSE – coincidence selection element, D_1, D_2 – discriminators, Amp – amplifier, ASE – anticoincidence selection element, TS – transmission system, Sc – scalar, N – corresponding mechanical counters, IP – transmission pulses, CA – anticoincidence circuit, CF – cathode follower.

The detecting telescopes were placed at 45, 75, 90, 120, 135, and 150° to the direction of the bremsstrahlung beam, and measurements were made simultaneously at two angles. Since the efficiencies of the two telescopes differed somewhat, the positions of the telescopes were interchanged at fixed time intervals, and the average readings of the two telescopes were used for each angle.

Cycles of measurements with hydrogen were alternated with measurements of the background. In experiments with the target empty, the average background for all angles was approximately 40% of the counting rate in the main experiments.

To check the stability of the operation of the entire setup, daily control measurements were made of the counting rate from a thick carbon target, both under the operating conditions and at the maximum bremsstrahlung energy, 265 Mev.

3. DETERMINATION OF THE TELESCOPE EFFICIENCY

To determine the differential cross sections from the measured yields of γp scattering, it is necessary to know the energy dependence of the efficiency of the telescopes employed for counting scattered γ quanta. We used in this investigation a method which we developed especially[10] to determine this dependence in the energy range from 35 to 150 Mev. This method is based on registration of the Compton scattering of the bremsstrahlung beam by electrons at a small angle (3°), for different maximum bremsstrahlung energies. The results of such a calibration are shown in Fig. 3.

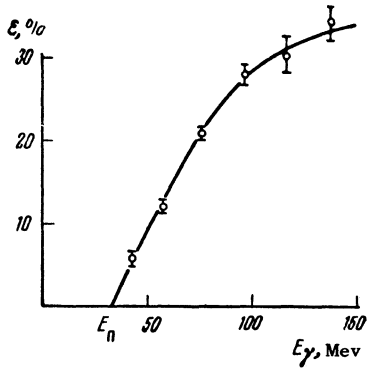

FIG. 3. Energy dependence of the efficiency of registration of γ quanta by the coincidence telescope (the errors are statistical).

The energy threshold of the telescope, $E_{thr} \approx 35$ Mev, calculated from the totality of the mean energy losses of the electrons leaving the converter, agreed with the experimentally obtained value.

An important factor was that in the calibration experiments, as in the main experiments, the entire working surface of the telescope was irradiated at once, since the telescope was located in these calibration experiments sufficiently far (11 m) from the carbon target (1.5 cm thick). In addition, the absolute bremsstrahlung flux was determined by the same methods as in the main experiments. The different errors in the determination of the absolute results of the main and calibration experiments were thus eliminated and our experiments yielded essentially a direct comparison of the differential angular cross sections for Compton scattering, known for the electrons and unknown for the protons.

4. REDUCTION OF THE EXPERIMENTAL DATA

The number of counts produced by a telescope located at an angle θ to the direction of the incident photon beam, referred to a definite number of counts of the monitor chamber, can be represented in the form

$$B = \iiint a\eta(E, E_{max})\,\varepsilon(E'(E, \theta))\,\frac{d\sigma}{d\Omega}(E,\theta)\,n_0 dV d\Omega\, dE, \quad (7)$$

where

$$a = E_{tot} \Big/ \int \eta(E, E_{max})\, EdE$$

is the γ-quantum flux (per unit area) averaged over the irradiated area; $\eta(E, E_{max})$ is the bremsstrahlung spectrum, $\epsilon(E')$ is the efficiency for registration of γ quanta of energy E' (which corresponds to the initial energy E) scattered at an angle θ, n_0 is the number of hydrogen nuclei per unit volume, dV is the element of working volume in the target; and $d\Omega$ is the solid angle "seen" by the telescope, corresponding to this volume.

The integral $J_\theta = \iint n_0 dV d\Omega$ is practically independent of the energy of a primary γ quanta.* This integral was calculated for each angle in accordance with the specific geometry of the experiment. To test the calculations, the ratio $J_\theta/J_{90°}$ was compared with the data obtained in an auxiliary experiment, in which the number of counts from a "point target" of PS-4 foamed polystyrol (a small cube 2 cm on each side) was compared with the number of counts from a cylinder of the same material, simulating the working volume of the liquid-hydrogen target.

Taking the cross section $\overline{d\sigma/d\Omega}$, averaged over the angles and energies, outside the integral sign, we obtain

$$\overline{d\sigma/d\Omega} = B/aJ_E J_\theta, \quad (8)$$

*The calculation of the absorption of γ quanta in the target will be discussed later on.

where

$$J_E = \int_{\text{thr}}^{E_{max}} \eta(E, E_{max})\, \varepsilon(E'(E, \theta))\, dE.$$

The bremsstrahlung spectrum of the synchrotron is given for a thick target by the Eyges formula, and a plot of $\epsilon(E')$ is shown in Fig. 3, where it is obvious that the integral J_E varies with the scattering angle θ because of the change in the energy of the scattered quantum. Figure 4 shows the products of the efficiency ϵ of registration of the scattered γ quanta and the distribution function η in the spectrum of the primary bremsstrahlung, for different scattering angles, as a function of the energy of the incident γ quanta. It is seen that the curves are approximately symmetrical and have a maximum near 56 Mev with an average half-width of approximately 25 Mev. The absolute value of J_E for 90° was computed graphically. The corrections for the change in the registration efficiency at different angles were also calculated graphically,

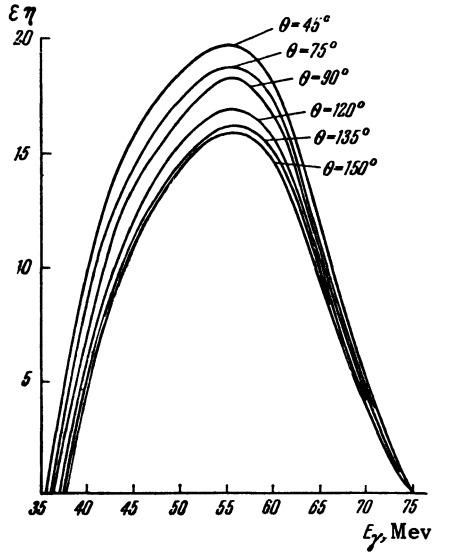

FIG. 4. The product of the registration efficiency of the scattered γ quantum and the distribution function in the spectrum of the primary bremsstrahlung (for different scattering angles).

from the ratio of the areas under the corresponding curves. They range from + 5% for 75° to - 15.4% for 150°.

The experimentally obtained differential cross sections for γp scattering at 45, 75, 90, 120, 135, and 150° are listed in the table (column 2). These results must be corrected for absorption in the target and for the contribution of the background processes.

Corrections for Absorption in the Target. Under the working conditions, some of the incident bremsstrahlung is absorbed in the walls and in the hydrogen of the target (~ 1.5%). The scattered radiation is also absorbed in amounts that vary with the angle, from 2.2% at 90° to 4.7% at 150°. The calculated corrections for the absorption of incident, scattered, and background γ quanta in the target are listed in column 3 of the table. Corrections for absorption in the paraffin filter and in the walls of the telescope were obviated by the fact that $\epsilon(E)$ was also measured in the presence of these absorbers.

Calculation of the Background. Since we did not separate the Compton γp scattering by registering the coincidence of the scattered γ quanta with the recoil protons, it was very important to allow for all possible background sources capable of making a noticeable contribution to the registration of γ quanta by a telescope with an approximate threshold of 35 Mev.

When a high registration threshold is obtained for both the telescope as a whole and for each individual counter (several Mev), it becomes impossible to register the Compton scattering of the γ quanta by the target electrons at large angles.

The single processes that produce high-energy quanta at the angles of interest to us are Delbruck scattering and radiative pair production. The cross section of Delbruck scattering[12] on hydrogen is small ($\sigma_{tot} \sim 10^{-34}$ cm^2), and this scattering has a strong forward orientation ($\sim 1/\theta^4$), so that it can be neglected completely even at 45°. According to estimates made by Feinman and Gomez,[13]

Angle θ, deg.	$10^{32}\frac{d\sigma}{d\Omega}(\theta)$, cm²/sr (without correction)	Correction for absorption of primary and registered γ quanta, $\Delta\sigma/\sigma$, %	Correction for extraneous processes (in units of 10^{-34} cm²/sr)				$10^{32}\frac{d\sigma}{d\Omega}(\theta)$, cm²/sr (final values)
			Rutherford scattering of electrons with subsequent radiation	Pair production at large angles with subsequent radiation	Emission of bremsstrahlung radiation at large angles	Total Correction	
45	4.66±0.28	+6.5	—127	—14.1	—5.4	—146	3.40±0.28
75	1.21±0.08	+3.5	—10.7	—1.4	—0.47	—12.6	1.12±0.08
90	1.14±0.05	+3.5	—6.7	—0.7	—0.3	—7.7	1.10±0.05
120	1.30±0.08	+4.5	—1.4	—0.18	—0.06	—1.6	1.34±0.08
135	1.48±0.08	+6.5	—0.89	—0.09	—0.04	—1.0	1.56±0.08
150	1.82±0.07	+6.5	—0.36	—0.04	—0.01	—0.4	1.93±0.07

the cross section for radiative pair production (production of a pair in the field of the nucleus with subsequent bremsstrahlung of one of the electrons in the same field) is approximately equal to the cross section $\sigma_{\gamma p}$ of the Compton γp scattering at a laboratory angle of 50° and E_γ = 40 Mev, but amounts to only ($\frac{1}{4}$) $\sigma_{\gamma p}$ at E_γ = 50 Mev. In view of the strong energy and angular ($\sim 1/\theta^4$) variations of the cross sections of this process, its total contribution at $E_\gamma \approx 56$ Mev and 75° is merely ~ 3% of the γp scattering. Since only a small part of the γ quanta emitted in radiative pair production has an energy greater than 35 Mev (threshold of our telescope), this process can be neglected at all angles except 45°. No corrections were therefore introduced for 75 — 150°, while the data for 45° were not used at all for further calculations of the polarizability of the proton, in view of the uncertainty in the value of the correction.

A background was produced also by multiple processes in the matter ahead of the target, in the target itself, and finally between the target and the first counter of the telescope, causing γ quanta of energies greater than 35 Mev to enter the telescope. To estimate the contribution of such processes, we calculated the number of high-energy electrons generated at small angles by Compton scattering and by pair production in the target and in the matter ahead of the target. We then considered a) the bremsstrahlung of these electrons at large angles in the direction of the counting channels (using Hough's data[14]), and b) their Rutherford scattering (using Mott's formula) in the direction of the counter channels with subsequent forward emission of bremsstrahlung in the matter ahead of the telescope. In addition, pair production at large angles in the hydrogen of the target[15] and the subsequent bremsstrahlung were considered. The results of the calculations are also listed in the table (columns 4 — 7).

The last column of the table gives the final values of the differential cross sections of γp scattering after making the corrections for the background processes and for absorption in the target. These final values are shown in Fig. 5 together with the data of other experimental investigations[16-18] for γ quanta of like energies (~ 60 Mev).

Systematic Errors. The tabulated errors in the determination of the γp scattering cross sections are due only to statistical errors of the main measurements. The principal possible source of systematic errors, namely the inaccuracy in the determination of the flux of the bremsstrahlung

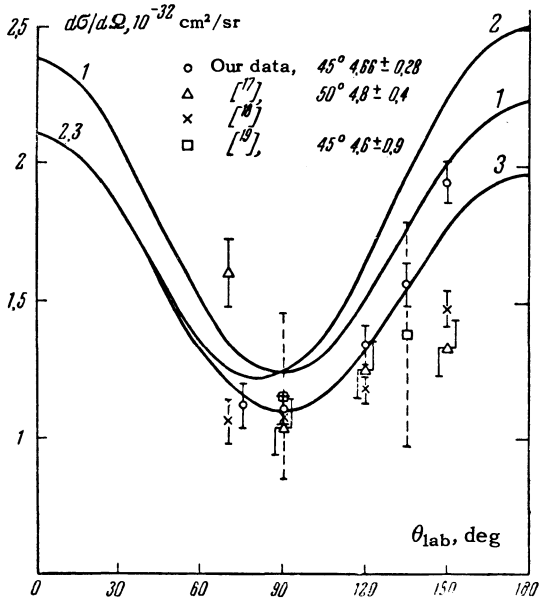

FIG. 5. Experimental data on γp scattering with ~60-Mev γ quanta. Curves — calculated: 1 — for $A_E = A_M = 0$; 2 — for $A_E = 0$, $A_M = 16$; 3 — for $A_E = 16$ and $A_M = 0$. The γp scattering cross sections compatible with the value $A_E + A_M = 16$ ($A_E, A_M > 0$) lies between curves 2 and 3 (θ — angle in the laboratory system).

quanta, is excluded because a direct comparison is used between the cross section of Compton scattering by protons and by electrons. Nevertheless, an error due to two inaccuracies in the determination of the product of the effective working volume of the target by the solid angle "seen" by the telescope, in the calibration and in the main (integral J_θ) experiments, does remain. We estimate this error to be ± 4%. In comparing the results of the calculation and the main experiments, additional errors of statistical origin arise, connected with the determination of the flux of γ quanta from the monitor counts in the two types of experiments and the summation of the dispersions of many points on the curve of the efficiency of registration of the γ quanta by the telescopes. The systematic errors due to the possible inaccuracy in the shape of the bremsstrahlung spectrum used in the calculations are of opposite signs in the calibration and in the main experiments, and are almost completely cancelled. The total value of the possible systematic error in the determination of the γp-scattering cross sections at angles from 75 to 150° is estimated at ±6%.

Returning now to the statistical errors listed in the table, we note that the errors for five experimental points range from +3.6 to +7.2%. The square root of the sum of dispersions for all five points equals 11.7%. Thus, when using the experimental points for comparison with the calculated curves (see

Fig. 5 curves 1-3), the mean statistical error calculated for an individual point is approximately 2.4%, while the total mean error (statistical plus systematic) is approximately 8%.

5. DETERMINATION OF PROTON POLARIZABILITY

To determine the electric and magnetic polarizability of the proton, we compare the results of Eq. (6) with those in the table and in Fig. 5. Even if we disregard the obviously excessive value of the γp-scattering cross section at 45°, we have five experimental values for the two parameters A_E and A_M of Eq. (6). It must be borne in mind, however that by far not all measurements of the angular distribution are equally sensitive to the values of A_E and A_M. As can be seen from (6), the forward-scattering (0°) cross section is a function of the sum of A_E and A_M, but not of each of these quantities individually:

$$\frac{d\sigma}{d\Omega}(0^\circ) = \frac{1}{2} r_0^2 \{2[1 - 2(A_E + A_M)\gamma^2] + 5.13\gamma^2\}. \quad (9)$$

On the other hand, the backward scattering, at 180°, depends only on the difference

$$\frac{d\sigma}{d\Omega}(180^\circ) = \frac{1}{2} r_0^2 \{2[1 - 4\gamma + 12\gamma^2 - 2(A_E - A_M)\gamma^2] + 78.39\gamma^2\}. \quad (10)$$

Our experiment yielded a γp-scattering pattern essentially only in the rear hemisphere, at laboratory angles from 75 to 150°. Using these experimental values only, we can obtain only A_E with a sufficient degree of determinacy, since γp-scattering cross sections at angles close to 90° are very insensitive to A_M. Using only the value

$$\frac{d\sigma}{d\Omega}(90^\circ) = (1.10 \pm 0.05) \cdot 10^{-32}\ \text{cm}^2/\text{sr}$$

we obtain

$$A_E = 16 \pm 5.8 \text{ or } \alpha_E = (11 \pm 4) \cdot 10^{-43}\ \text{cm}^3$$

We can make use of the dispersion relation as an additional source of information to account for the forward γp scattering, which was not measured experimentally, and thus obtain a better value of α_E and and estimate of the magnetic polarizability α_M.

Cini and Stroffolini[19] have shown that the cross sections of forward γp scattering $(d\sigma/d\Omega)$ (0°) are completely determined at energies below the photomeson threshold by the total cross sections, obtained directly by experiment, of the photoproduction of pions induced by unpolarized γ quanta, and that separate meson photoproduction cross sections for γ quanta polarized parallel and antiparallel to the proton spin need be known for the calculation of $(d\sigma/d\Omega)$ (0°) only at higher energies. Using the relations given by Bernardini[20] we obtain

$$\frac{d\sigma}{d\Omega}(0^\circ) = \left[\frac{e^2}{Mc^2} - \frac{\gamma^2}{4\pi^2}\left(\frac{\hbar}{Mc}\right)^{-1} \int_0^\infty \frac{\sigma_p(\gamma') + \sigma_a(\gamma')}{\gamma'^2 - \gamma^2} d\gamma'\right]^2 + \gamma^2\left[\frac{\lambda_a^2}{2}\frac{e^2}{Mc^2} - \frac{\gamma^2}{4\pi^2}\left(\frac{\hbar}{Mc}\right)^{-1} \int_0^\infty \frac{\sigma_p(\gamma') - \sigma_a(\gamma')}{\gamma'(\gamma'^2 - \gamma^2)} d\gamma'\right]^2 + \gamma^2 \frac{1}{32\pi^2}\left(\frac{\hbar}{Mc}\right)^{-2} [\sigma_p^2(\gamma) + \sigma_a^2(\gamma)], \quad (11)$$

where $\sigma_p(\gamma)$ and $\sigma_a(\gamma)$ are the total cross sections for the photoproduction of pions on protons for γ quanta of energy γMc^2 (laboratory system), polarized parallel and antiparallel to the proton spin, respectively. The sum $\sigma_p(\gamma) + \sigma_a(\gamma) = \sigma_t(\gamma)$ is the total photoproduction cross section for an unpolarized beam of γ quanta.

The last term vanishes below the photoproduction threshold and we have, accurate to terms of order γ^2,

$$\frac{d\sigma}{d\Omega}(0^\circ) = r_0^2 \left\{1 - \left[\frac{1}{2\pi^2}\left(\frac{e^2}{\hbar c}\frac{\hbar}{Mc}\right)^{-1} \int_0^\infty \frac{\sigma_\pi(\gamma') + \sigma_a(\gamma')}{\gamma'^2 - \gamma^2} d\gamma' - \frac{\lambda_a^4}{4}\right]\gamma^2\right\}. \quad (12)$$

Comparing (12) and (9) (bearing in mind that the very definition of polarizability applies to quanta of zero energy) and going from A_M and A_E to α_M and α_E, we obtain

$$\alpha_E + \alpha_M = \frac{1}{4\pi^2}\frac{\hbar}{Mc} \int_0^\infty \frac{\sigma_t(\gamma)}{\gamma^2} d\gamma. \quad (13)$$

It is obvious that as long as α_E and α_M are positive, (13) characterizes the upper limit of the values of each of the two proton polarizabilities.

Using the latest data on the photoproduction of $\pi^\pm$ mesons[20] and π^0 mesons[21,22] (see Fig. 6), we obtain $\alpha_E + \alpha_M = 11 \times 10^{-43}\ \text{cm}^3$, i.e., $A_E + A_M = 16$.

Inasmuch as (13) is obtained from the most general properties of the scattering matrix, there are no reasons to cast any doubts on it at all. Therefore, provided (6) is correct, i.e., provided the scattering theory used here is valid with sufficient accuracy there is no need for taking into account higher powers of the γ-quantum frequency, we can readily establish the limits of the γp-scattering cross sections for all angles. If A_E and A_M are positive, and if $A_E + A_M = 16$, these limits are the curves obtained from (6) at $A_E = 0$, $A_M = 16$ and $A_E = 16$, $A_M = 0$. It is seen from Fig. 5, where the values of $(d\sigma/d\Omega)$ (θ) compatible with $A_E + A_M = 16$ lie in the region between curves 2 and 3, that all our experimental data for

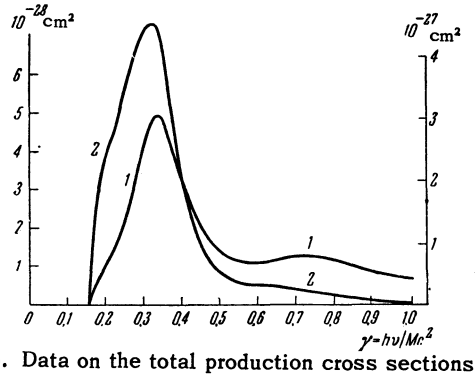

FIG. 6. Data on the total production cross sections of π^+ and π^0 mesons on protons, employed in determining the sum of electric and magnetic polarizability of the proton. Curve 1 – the value of $\sigma_{\pi^0} + \sigma_{\pi^+}$ (left-hand scale); curve 2 – the value of $(\sigma_{\pi^0} + \sigma_{\pi^+})\gamma^2$ (right-hand scale).

75 – 150° fall in this region, while the values obtained in references 16 – 18 for the γp-scattering cross sections in the backward hemisphere are somewhat too low.

Using $A_E + A_M = 16$ and calculating the value of A_E by the method of least squares to give best agreement with our results, we obtain $A_E = 13 \pm 3$ and $A_M = 3 \pm 3$, while the sum of the weighted squares of the errors is $D = 1.8 \times 10^{-66}\,\text{cm}^4 \cdot \text{sr}^{-2}$.

We thus conclude that

$$\alpha_E = (9 \pm 2) \cdot 10^{-43}\,\text{cm}^3, \quad \alpha_M = (2 \mp 2) \cdot 10^{-43}\,\text{cm}^3.$$

6. DISCUSSION OF THE RESULTS

The magnetic polarizability of the proton, as already indicated by Baldin,[6b] is thus much less than the electric polarizability. A determination of the magnetic polarizability of the proton is more sensitive to a possible contribution to the γp-scattering cross section from terms proportional to higher powers of the γ-quantum frequency (greater than γ^2), and therefore a detailed analysis of the role of these terms is of interest if a more refined value of A_M is desired. As regards the electric polarizability, we see not only that the sum $A_E + A_M$ agrees with our experimental data, but the optimal value $A_E = 13 \pm 3$ agrees within the limits of errors with the value obtained above from the cross section for scattering at 90° ($A_E = 16 \pm 5.8$).

A direct comparison of the experimental results with the curve obtained from (1) (without allowance of the polarizability of the proton) gives a much larger sum of weighted squares of errors, $D = 10.3 \times 10^{-66}\,\text{cm}^4\text{sr}^{-2}$, than obtained with (6). The best agreement with (1) is obtained by increasing all the experimental cross sections by 8%; this, however, is at the border of possible systematic errors.

The question of electric polarizability of nucleons has been extensively discussed in the literature of late in connection with the development of theoretical ideas[23,24] on the role of polarizability of neutrons electrically scattered by small angles in the Coulomb field of heavy nuclei. The electrical polarizability of the neutron $(\alpha_E)_n = (8 \pm 3.5) \times 10^{-41}\,\text{cm}^3$, calculated by Aleksandrov[25] from an analysis of the data on neutron scattering, certainly contradicts the totality of data on the scattering of γ quanta and photoproduction of π mesons, a fact noted in the theoretical papers[7,26-30] and now again confirmed in our experiments.

The last analysis of the new experiments on neutron scattering[28] has led, to be sure, to a reduction in the limiting value of α_E, namely $0 < (\alpha_E)_n < 2 \times 10^{-41}\,\text{cm}^3$, but does not give any more definite results. As long as $\alpha_E \sim 10^{-42}\,\text{cm}^3$, neutron experiments can hardly establish quantitatively the contribution of the electric polarizability. The main path towards determining the electric and magnetic polarizability of the nucleon – properties due to the change in the structure of the meson cloud in the nucleon – lies therefore in a study of the meson processes and primarily the photoproduction of pions and the nucleon Compton effect.

Rough estimates of the electric polarizability of the neutron based on meson theories, yield a quantity on the order of[26,28]

$$(e^2/\hbar c)\,(f^2/\hbar c)\,(\hbar/\mu c)^3 = 1.6 \cdot 10^{-42}\,\text{cm}^3,$$

where $(f^2/\hbar c) = 0.08$. A result close to this estimate $(\alpha_E)_n = (1.6 \text{ to } 1.8) \times 10^{-42}\,\text{cm}^3$ was obtained[26] by calculating the polarizability of the meson cloud in a nucleon, with the aid of the Chew theory for functions with Gaussian and exponential forms, with a cutoff parameter $5.6\ \mu c/\hbar$.

In analyzing the data on pion photoproduction and γp scattering, Baldin[6] obtained for the lower limit of nucleon polarizability (assuming single-meson exchange only) a value $(\alpha_E)_p = 4 \times 10^{-43}\,\text{cm}^3$. The upper limit of $(\alpha_E)_p$, derived by him by assuming nearly equal values for the γp-scattering cross section at 90° and the Thompson cross section $(r_0^2/2)$, is estimated at $1.4 \times 10^{-42}\,\text{cm}^3$. From the data on pion photoproduction, Breit and Rustgi[29] obtained a similar estimate, $(\alpha_E)_n \lesssim 2 \times 10^{-42}\,\text{cm}^3$.

It must be borne in mind that, because the cross section σ^- of the process $\gamma + n \to \pi^- + p$ exceeds near the threshold the cross section σ^+ of the process $\gamma + p \to \pi^+ + n$, and because of the considerable contribution of the threshold region to the dispersion integral (13), the electric polar-

izability of the neutron should be 20 or 30% greater than the corresponding value for the proton.[6b,29] As is clear from our calculations with Eq. (13), the upper limit for the electric polarizability of the proton can be reduced to $(\alpha_E)_p = 1.1 \times 10^{-42}\,cm^3$.

To arrive at our final conclusions regarding the value of $(\alpha_E)_p$, we used also the calculated limiting value of the sum $(\alpha_E + \alpha_M)_p = 1.1 \times 10^{-42}\,cm^3$; however, even the direct results of the experiments confirm in general our various theoretical estimates of $(\alpha_E)_p$.

In conclusion, let us consider the problem of the mean-square fluctuation $(\overline{r^2})^{1/2}$ of the displacement of the center of distribution of the electric charge in the polarized proton about its center of gravity, associated with α_E.

According to references 6 and 29, this value is connected with the electric polarizability of the proton by the usual relation

$$(\overline{r^2})^{1/2} = \left[\tfrac{3}{2}\alpha_E (e^2/\hbar c)^{-1} \Delta E/\hbar c\right]^{1/2}, \qquad (14)$$

where ΔE is the energy difference between the ground and the polarized states of the proton. Since the polarization is due to the excitation of the meson cloud or to the occurrence of a resonant isobar state, a suitable choice of ΔE lies between μc^2 and $2\mu c^2$.

For $\alpha_E = 9 \times 10^{-43}\,cm^3$ we obtain from (14), for the proton, the mean-squared fluctuation of the length of the induced electric dipole

$$(\overline{r^2})^{1/2} = 3.5 \text{ to } 5 \cdot 10^{-14}\,cm.$$

It is undoubtedly desirable to develop a more detailed theory of magnetic polarizability of the proton, so as to relate the values of α_E and α_M with the contributions from different mechanisms of pion photoproduction, to obtain theoretical limits for α_M, and to compare them with experiment, and also to compare the fluctuations of the lengths of electric and magnetic nucleon dipoles.

The authors express warm gratitude to S. P. Balat'ev, R. G. Vasil'kov, E. V. Minarik, and A. Samiullin for help with the experiments, and to G. Ivanov for active participation in the reduction of the results. It is also our pleasure to thank the entire synchrotron crew for help in many hours of experiments and express sincere gratitude to A. M. Baldin and V. N. Gribov for participating in discussion of the results of the work.

Note added in proof (May 20, 1960). V. N. Gribov has advised us that the roles of the different factors in the quadratic (in the frequency) terms of the amplitude of Rayleigh (E1) scattering (see Introduction) are made clear by the following expression for this amplitude (in units e^2/Mc^2):

$$R = (1 - A_E\gamma^2)(ee') = \left\{1 - \left[\tfrac{1}{3}r_e^2\left(\frac{Mc}{\hbar}\right)^2 + \tfrac{1}{4} + \frac{\gamma_a}{2} + A_E^*\right]\gamma^2\right\}(ee'),$$

where **e** and **e'** are unit vectors in the direction of polarization of the incident and scattered protons, r_e is the electric radius of the proton, A_E^* is a measure of polarizability analogous to our A_E but now in its usual sense.

[1] J. L. Powell, Phys. Rev. **75**, 32 (1949).
[2] M. Gell-Mann and M. Goldberger, Phys. Rev. **96**, 1433 (1954).
[3] F. E. Low, Phys. Rev. **96**, 1428 (1954).
[4] A. Klein, Phys. Rev. **99**, 998 (1955).
[5] R. Capps, Phys. Rev. **106**, 1031 (1957).
[6] A. M. Baldin, a) Paper at Conference on Elementary Particles, Padua-Venice, 1957 b) Nucl. Phys. in press.
[7] E. C. Park, J. Sci. Instr. **33**, 257 (1956).
[8] Barber, George, and Reagan, Phys. Rev. **98**, 73 (1955).
[9] P. S. Baranov, Dissertation, Phys. Inst. Acad. Sci. 1955.
[10] Gol'danskiĭ, Karpukhin, and Pavlovskaya, Приборы и техника эксперимента (Instrum. and Meas. Techniques), No 3, 1960.
[11] L. Eyges, Phys. Rev. **81**, 982 (1951).
[12] A. I. Akhiezer and V. B. Berestetskiĭ, Квантовая электродинамика (Quantum Electrodynamics), Fizmatizdat, 1959.
[13] L. G. Hyman, Mass. Inst. Tech. PhD Thesis, 1959.
[14] P. V. C. Hough, Phys. Rev. **74**, 80 (1948).
[15] R. C. Miller, Phys. Rev. **95**, 796 (1954).
[16] C. Oxley and V. L. Telegdi, Phys. Rev. **100**, 435 (1955).
[17] C. Oxley, Phys. Rev. **110**, 733 (1958).
[18] Pugh, Gomez, Frisch, and Janes, Phys. Rev. **105**, 982 (1957).
[19] M. Cini and R. Stroffolini, Nucl. Phys. **5**, 684 (1958).
[20] G. Bernardini, Paper at Ninth International Conference on High-Energy Physics, Kiev, 1959.
[21] Vasil'kov, Govorkov, and Gol'danskiĭ, JETP **37**, 11 (1959), Soviet Phys. JETP **10**, 7 (1960); Nucl. Phys. **12**, 337 (1959).
[22] K. Berkelman and J. Waggoner, Phys. Rev. in press.
[23] Yu. A. Aleksandrov and I. I. Bondarenko, JETP **31**, 726 (1956), Soviet Phys. JETP **4**, 612 (1957).
[24] Barashenkov, Stakhanov, and Aleksandrov, JETP **32**, 154 (1957), Soviet Phys. JETP **5**, 144 (1957).

[25] Yu. A. Aleksandrov, **33**, 294 (1957), Soviet Phys. **6**, 228 (1958).
[26] W. S. Barashenkov and B. M. Barbashov, Nucl. Phys. **9**, 426 (1958).
[27] Blokhintsev, Barashenkov, and Barbashov, Usp. Fiz. Nauk **68**, 417 (1959), Soviet Phys. Uspekhi **2**, 505 (1960).
[28] R. M. Thaler, Phys. Rev. **114**, 827 (1959).
[29] G. Breit and M. L. Rustgi, Phys. Rev. **114**, 830 (1959).
[30] L. L. Foldy, Phys. Rev. Lett. **3**, 105, 1959.

Translated by J. G. Adashko
330

Errata

Volume	No.	Author	page	col.	line	Reads	Should read
10	5	Bogachev et al.	872	l	21	± 0.3 cm	± 0.7 cm
11	6	Gol'danskii et al.	1229	r	Eq. (13)	$\frac{1}{4\pi^2}\ \frac{h}{Mc}$	$\frac{1}{4\pi^2}\ \frac{h}{Mc}$
			1331	r	4	$\ldots + \frac{1}{4} + \frac{\gamma_a}{2}$	$\ldots + \frac{1}{4}\cos\ + \frac{\lambda}{2}$
12	2	Moroz and Fedorov	210	l	Eq. (7)	$\ldots \frac{\sin k_0 x_0}{k_0}\, e^{i\mathbf{kx}} d^3k,$	$\ldots \frac{ik_0\delta(k^2)}{\lvert k_0\rvert} e^{ikx}\, d^4k,$
			212	l	Eq. (39)	$\ldots = 4\pi\hbar c \ldots$	$\ldots = -4\pi\hbar c \ldots$
			212-3	r-l	Eqs. (44) and (39)	$\ldots + \frac{1}{2} iel\, \nabla_k \psi_4(x) \ldots$	$\ldots + \frac{1}{2} iel \nabla_k \psi_4''(x) \ldots$
			213	r	Eq. (51), line 2	$\ldots \frac{iel}{2} \int \nabla_m \psi_4(x) \ldots$	$\ldots \frac{iel}{2} \int \nabla_m \psi_4''(x) \ldots$
			213	r	Eq. (53)	$\ldots e^{-ik_0 \lvert x_0 - x_0' \rvert} e^{i\mathbf{k}(\mathbf{x}-\mathbf{x}')} \frac{d^3k}{k_0}.$	$\ldots e^{ik(x-x')} \frac{d^4k}{2\pi i (k^2 - i\varepsilon)}$
12	3	Nikishov	530	l	Eq. (10)	—	$\mu^{(2)} = \frac{1}{2\beta_2 \xi} \ln\left[\frac{y_1 - 1}{y_1 + 1} \cdot \frac{-y_2 - 1}{-y_2 + 1}\right]$
			533	r	Fig. 4	The dashed curve of Fig. 4 has been incorrectly calculated (corrections to μ^+ scattering on electrons). Its value ranges from −6 to −8.	
12	1	Anisovich	72, 75		Eqs. (4a), (4b), (11)	$\sigma(\pi^+ + p \to n + \pi^+ + \pi^+)$	$2\sigma(\pi^+ + p \to n + \pi^+ + \pi^+)$
	5	,,	948		Eq. (6)	$\sigma(\pi^- + p \to n + \pi^0 + \pi^0)$	$2\sigma(\pi^- + p \to n + \pi^0 + \pi^0).$